



CONDITION MONITORING OF A WORM-TYPE GEARBOX IN TERMS OF TRIBO-PROGNOSTICS THROUGH VIBRO-THERMAL ANALYSIS

S.Seckin EROL¹, Michael G. PECHT²

¹ Kilis 7 Aralik University, Faculty of Engineering and Architecture, Mechanical Engineering Dept., 79000 Kilis-Turkey

² University of Maryland, Center for Advanced Life Cycle Engineering, College Park, MD 20742 USA

Corresponding author: S.Seckin EROL, E-mail: sserol@kilis.edu.tr

Abstract. Thermal technique can augment vibration analysis in an approach called vibro-thermal analysis, which is developed in this study. Vibro-thermal analysis is appropriate especially for large machines in enterprises and for the aviation industry. This study designed a test setup located in laboratory conditions to investigate the effects of oil starvation under different loads on a worm-type gear using a new perspective called tribo-prognostics. The main purpose of the study is to introduce this new prognostics and health management (PHM) approach. Thermal data, infrared distribution and quantitative charts were considered for thermal analysis; and spectrum data, waterfall data and quantitative charts were considered for vibration analysis. Tribo-prognostics was efficiently implemented by detecting oil starvation through a symptomatic level of the condition monitoring. Vibro-thermal analysis uses vibration and thermal monitoring to reduce the errors in data interpretation for predictive maintenance practices. The health of a gearbox can be assessed by vibration analysis of a bearing; and gear vibration frequencies become more prominent when the load and oil insufficiency are increased. Thermal monitoring assists vibration analysis with respect to the overall mapping of the inspected system and can help assess system health more quickly. This paper shows that vibro-thermal analysis is a viable supplementary model of vibration and thermal analysis.

Key words: prognostics, thermal analysis, tribology, vibration, predictive maintenance.

1. INTRODUCTION

Gearboxes have been used in transportation vehicles, manufacturing machines, heating-plumbing services and for many other transmission purposes since they were invented. This study investigated worm gears using condition monitoring techniques such as vibration and thermal analysis. Asset health management with condition monitoring can ensure sustainable nominal functionability and can protect capital investment. Other advantages of condition monitoring include enhanced human safety, fewer spare parts to stock, less time loss, higher quality, and fewer maintenance activities. Predictive maintenance technologies must be constantly improved to increase the efficiency of sustainable machine health.

This paper conducted a comparative study that monitored the condition of worm gears under different phenomena using vibration and thermal analysis and results are presented for sustaining the health of gear mechanisms in that research. Vibro-thermal model is based on comparison of vibration and thermal analysis as complement of each other for increasing the sensitivity of the acquired data. The principles of friction, wear and lubrication have been studied in tribology science, and prognostics is the stage where the physical symptoms of machine health are monitored before any failure occurs. The tribo-prognostic approach has been used to monitor the condition of systems at a prognostic level in terms of friction, wear, and lubrication.

Gearboxes are widely used in industrial enterprises especially for power transmission. Lamani et al. [1] reported that there is, however, a research gap in vibration analysis for worm-type gearboxes. Gear failures at the initial stage may decrease the transmission quality and cause high-amplitude vibrations and noise in rotating machines. Consequently, condition monitoring of gearboxes is crucial in order to prevent critical breakdowns and human injuries [2]. Sait and Sharaf-Eldeen [3] reviewed the literature on changes in condition monitoring of rotating machines. Mechanical failures have mainly been studied with vibration analysis. Mauricio et al. [4] conducted research on gearboxes with healthy, chipped and missing teeth. They implemented vibration analysis on different signal processing techniques such as envelope analysis, spectral

correlation, principal component analysis and linear discriminant analysis. The main faults in worm gears are scoring, plastic flow, fracture, pitting and wear. Ghodake et al. [5] stated that vibration analysis and wear debris analysis together give the best results in detection of failures for worm-type gearboxes. Al-Arbi [6] concluded that waveform analysis is not sufficient for prognosis or diagnosis of gear failures with respect to the vibration analysis of gears. Spectrum analysis is more reliable in detection of gear failures than time domain analysis but operating conditions may affect the evaluation results. Vibration signals are affected by the reactional response on the gearbox case and motor element. Vecer et al. [7] conducted research on condition indicators (CIs) for monitoring gearboxes by vibration signals. They reported that wear on the gearbox might be hidden in vibration data by the noise and suggested extra techniques in support of their analysis. Yin et al. [8] developed a statistical model of a synchronous signal average in order to inspect healthy; or faulty gears and gear failures. They studied statistical modeling of gear vibration signals and its application to detection and diagnosis of gear faults.

In this study, a test setup was designed for studying artificial and spontaneous failures through gears and bearings. Comparison of vibration versus thermal analysis was conducted in order to monitor the conditions of a worm-type gearbox. An increase in the efficiency of condition monitoring was proposed based on the usage of vibration and thermal analysis together. The tested system has been inspected in a prognostic state with a tribological perspective. This study aims to assess the efficiency of vibro-thermal analysis on a worm-type gearbox with the tribo-prognostic approach.

2. MATERIALS AND METHODS

The test setup in Fig. 1 was located in laboratory ambient conditions and was consisted of a frequency inverter, a computer with a high-capacity processor and test setup components. The test setup was designed with respect to possible gearbox and bearing failures. Two shafts supported with four ball bearings were linked by belt-pulley. One shaft was driven by a worm-type gearbox coupled with a triphase electrical motor, while the other shaft was connected to an adjustable mass. The shaft rotation speed was determined with the electrical frequency inverter. A triaxial vibration sensor based on micro-electro-mechanical system (MEMS) technology was used to acquire vibration signals and a thermal camera was used for gathering temperature and heat data through the test setup under the test conditions.

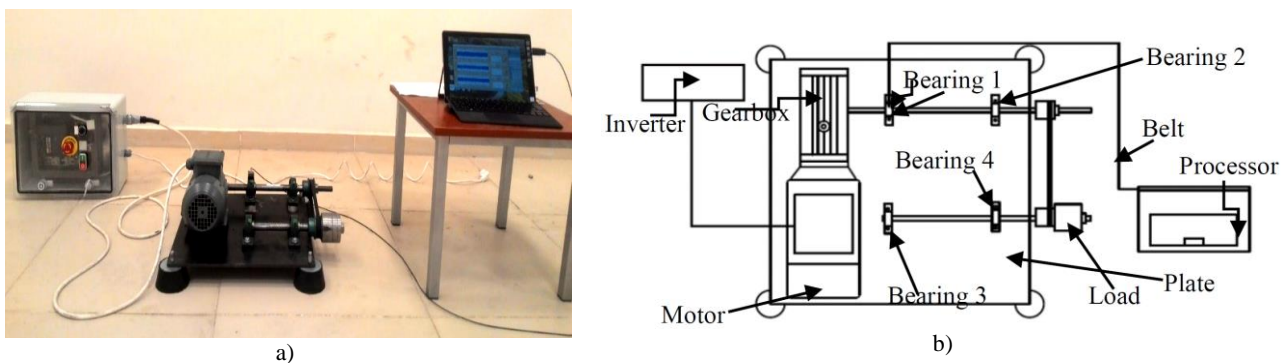


Fig. 1 – Test setup: a) Actual view, b) Schematic view.

A vibration sensor was mounted with a magnetic base over the measuring location at bearing 1 (Fig. 1) and coupled with a powerful computer processor in order to transfer data for analysis. The thermal camera stored the data in internal memory for transferring to the computer. In this study, tests were implemented under three main conditions. The first condition consisted of an electrical motor-driven unused worm-type gearbox tested by a vibro-thermal condition monitoring system with 250 g load and 1 000 g load. The second condition consisted of an electrical motor-driven oil-removed worm-type gearbox tested by vibro-thermal condition monitoring system with 1 000 g load. The third condition consisted of tests implemented under the electrical frequency of 32.7 Hz set over an inverter in order to determine the rotation speed of the electrical motor and the gearbox. The characteristic vibration signal frequencies were estimated with respect to the gear features based on rotation frequencies, and the number of teeth in order to analyze and evaluate vibration signals. The gearbox vibration frequencies were as follows:

• Gear frequency, $f_g = r_g / 60$ (Hz) : 4.4 Hz	<ul style="list-style-type: none"> • Number of teeth on pinion..... n_p • Pinion speed, rpm..... r_p • Number of teeth on gear..... n_g • Gear speed, rpm..... r_g • Ratio, n_g/n_p or r_p/r_g m_g
• Pinion frequency, $f_p = r_p / 60$ (Hz) : 33 Hz	
• Tooth mesh frequency, $f_m = f_p \cdot n_p = f_g \cdot n_g$ (Hz) : 132 Hz	
• Assembly phase frequency, $f_a = f_m / n_a$ (Hz) : 66 Hz n_a : product of common prime factors : 2	
• Tooth repeat frequency, $f_{tr} = (f_m \cdot n_a) / (n_g \cdot n_p)$ (Hz) : 2.2 Hz	

Vibration frequencies for bearing components are another source of signals in the spectrum findings besides gear vibration frequencies. These frequencies were also estimated in order to give more depth to the vibration signal analysis. The bearing dimensions were as follows: diameter of ball (r): 8.4 mm, number of balls (n): 8, pitch diameter (d): 33.5 mm, contact angle (β): 0° . The bearing frequencies were as follows:

- Ball pass frequency of outer ring, $f_{bpfo} = f(n/2) [1 - (r/d)\cos\beta]$: 13.187 Hz;
- Ball pass frequency of inner ring, $f_{bpfi} = f(n/2) [1 + (r/d)\cos\beta]$: 22.013 Hz;
- Ball spin frequency, $f_{bsf} = f(d/2r) [1 - (r/d)\cos\beta]$: 8.222 Hz;
- Cage frequency, $f_c = f/2 [1 - ((r/d)\cos\beta)^2]$: 1.648 Hz.

A model was proposed on vibration data with thermal inspection may help for less sophistication in analyzing condition of the machine rather than a singular technique [9]. We identify the diagnosis methodology implemented for different levels of failure conditions in gears with vibration and thermal matrix [10]. The methodology is mainly consists of four steps. The first step is designing an experimental setup and artificial failure conditions; second is data acquisition; third is analysis between vibration and thermal data; and the last step is conclusion of the effectiveness in vibro-thermal technique.

3. DATA ACQUISITION AND ANALYSIS

Tests were implemented under vibration data acquisition in three axes as X , Y , Z and the data analysis was implemented for the Y axis in this study whereas signals were more dominant. Resonance phenomena were detected in the vibration spectrums and the natural frequency is symbolized with f_n . Comparisons of the statistical data for the X , Y , Z axes are given as well in Section 4. Thermal data were captured in each test and inspections are given with the experimental findings.

a. Condition of sufficient oil under 250 g load. In this part, experimental data are given with respect to the vibration and thermal analysis for the condition of sufficient oil under 250 g load. Vibration data were inspected through spectrum domain and table of dominant signals; thermal data were inspected with an infrared perspective with respect to the temperatures. Figure 2a shows the vibration frequency spectrum. The signal at a bearing frequency of $104 \times f_{bsf}$ excited the natural frequency at 854 Hz, and subharmonic resonance signal occurred with the highest amplitude of 0.62 m/s^2 , which is indicated in Table 1.

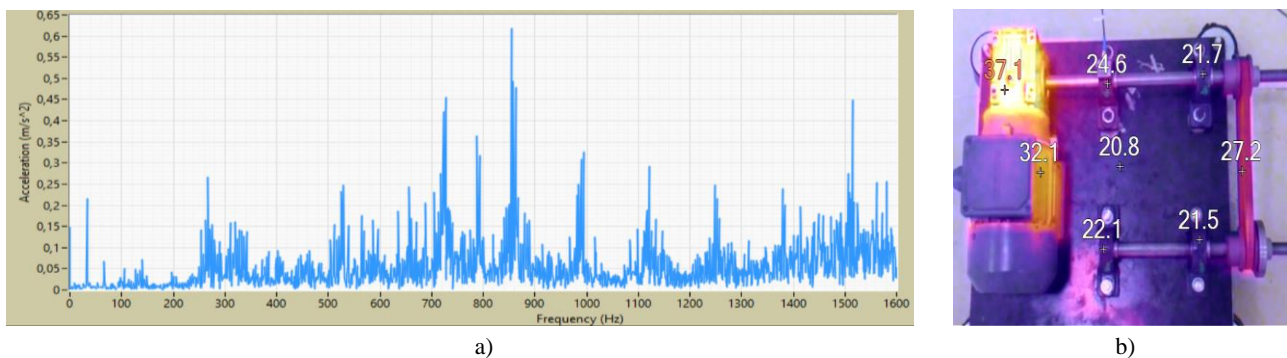


Fig. 2 – a) Spectrum domain for condition of sufficient oil with 250 g load; b) thermal inspection for condition of sufficient oil with 250 g load.

The second dominant signal was detected at 858 Hz and was excited by the vibration signal at $13 \times f_a$. The third dominant signal appeared at $105 \times f_{bsf}$. The fourth dominant signal was a natural frequency at 727 Hz that was excited by the vibration signal at $55 \times f_{bpfo}$. The fifth dominant signal is appeared on natural frequency at 1 515 Hz excited by $115 \times f_{bpfo}$. The sixth dominant signal appeared on a natural frequency at 788 Hz as well as excited by $96 \times f_{bsf}$. The sum of the six dominant amplitudes has been estimated as 2.87 m/s^2 . Mesh frequency (f_m) was obtained at 132 Hz with the amplitude of 0.023 m/s^2 which means that the gear system is in a healthy condition in low amplitude with respect to Fig. 2. The signal on the second order of mesh frequency was detected at 264 Hz with the amplitude of 0.05 m/s^2 . The fundamental frequency of the pinion ($1 \times f_p$) was obtained at 33 Hz with the amplitude of 0.22 m/s^2 .

Table 1

Dominant frequencies in condition of sufficient oil with 250 g load (s: signal)

1.S	2.S	3.S	4.S	5.S	6.S
f_n	f_n	$105 \times f_{bsf}$	f_n	f_n	f_n
$(104 \times f_{bsf})$	$(13 \times f_a)$		$(55 \times f_{bpfo})$	$(115 \times f_{bpfo})$	$(96 \times f_{bsf})$

Under the condition of sufficient oil with 250 g load, the findings obtained by waterfall data show that high-amplitude vibrations accumulated between 350 Hz and 500 Hz. Some peaks can also be seen around 150 Hz and 800 Hz. Thermal heat distribution and actual temperatures are indicated on vibration measurement points in Fig. 2b.

The highest temperature was detected on the gearbox in the amount of 37.1°C . The measured temperature of bearing 1 with 24.6°C is higher than the measured temperature of bearings 2, 3, and 4. Overheated regions are located around the gearbox and electrical motor.

b. Condition of sufficient oil under 1 000 g load. This part gives experimental data with respect to the vibration and thermal analysis for the condition of sufficient oil under 1 000 g load. Vibration data was inspected through spectrum domain and table of dominant signals; thermal data was inspected over infrared perspective with respect to the temperatures.

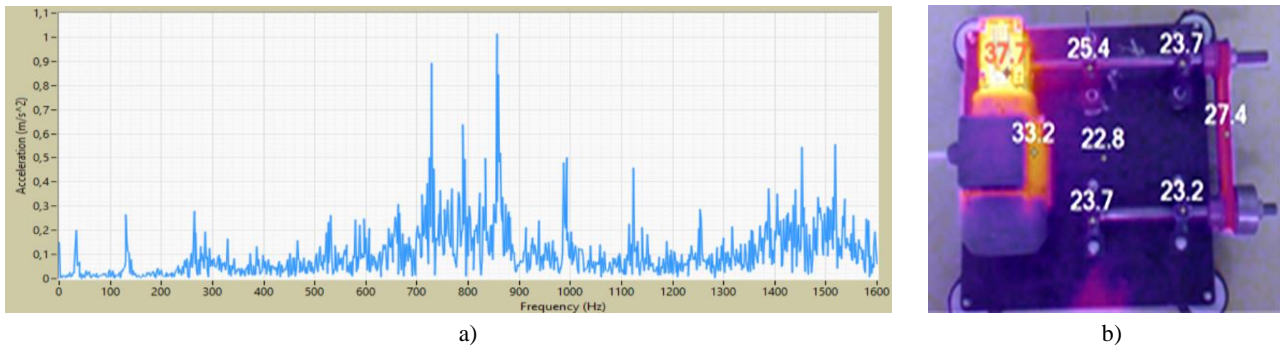


Fig. 3 – a) Spectrum domain for condition of sufficient oil with 1 000 g load; b) thermal inspection for condition of sufficient oil with 1 000 g load.

Figure 3a shows the vibration frequency spectrum. In Table 2, the signal at 855 Hz has been excited by a bearing frequency of $104 \times f_{bsf}$ and resonance occurred with the highest amplitude of 1 m/s^2 . The second dominant signal appeared at a natural frequency of 728 Hz that was excited by $442 \times f_c$. The third dominant frequency appeared at a bearing component frequency of $105 \times f_{bsf}$. The fourth dominant signal is a natural frequency at 790 Hz that was excited by $96 \times f_{bsf}$. The fifth dominant signal is a natural frequency as well at 1 518.5 Hz excited by $69 \times f_{bpfi}$. The sixth dominant signal is detected at a pinion frequency of $1 \times f_p$ with the amplitude of 0.19 m/s^2 . The sum of the six dominant amplitudes is 3.95 m/s^2 . The mesh frequency ($1 \times f_m$) was detected at 132 Hz with the amplitude of 0.2 m/s^2 with respect to Figure 6. A signal occurred at the second order of the mesh frequency and its amplitude was 0.28 m/s^2 . The amplitude of $1 \times f_m$ has been increased with respect to the increase in the load; and the amplitude of $2 \times f_m$ is higher than $1 \times f_m$ which means there is an excessive misalignment on the gear system.

Table 2

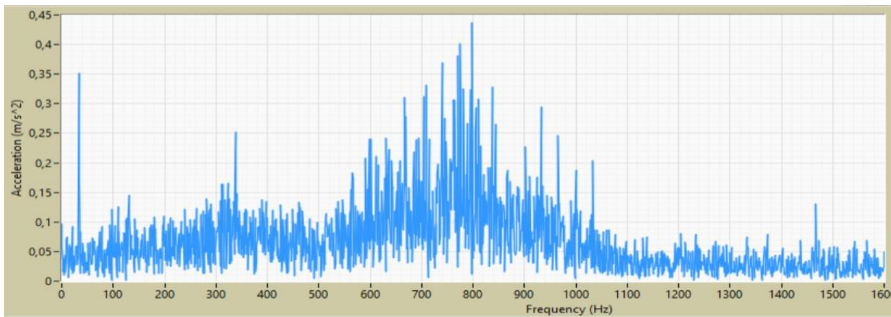
Dominant frequencies in condition of sufficient oil with 1 000 g load (s: signal)

1.S	2.S	3.S	4.S	5.S	6.S
f_n ($104 \times f_{bsf}$)	f_n ($442 \times f_c$)	$105 \times f_{bsf}$	f_n ($96 \times f_{bsf}$)	f_n ($69 \times f_{bpf}$)	$1 \times f_p$

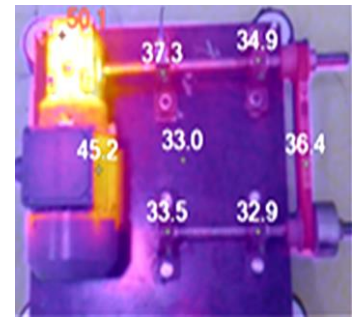
Under the condition of sufficient oil with 1 000 g load, the findings of the relevant waterfall data indicate that high-amplitude vibrations accumulated between 350 Hz and 450 Hz. Some peaks can also be seen around 750–800 Hz. Thermal heat distribution and actual temperatures are indicated on vibration measurement points in Fig. 3b.

The highest temperature was detected on the gearbox at 37.7 °C. The measured temperature of bearing 1 at 25.4 °C was higher than the measured temperature of bearings 2, 3, and 4.

c. Condition of insufficient oil under 1000 g load. In this part, experimental data is given with respect to the vibration and thermal analysis for the condition of insufficient oil under 1 000 g load. Vibration data was inspected through the spectrum domain and table of dominant signals; thermal data was inspected with an infrared perspective with respect to the temperatures. Vibration frequency spectrum is given in Fig. 4a, and higher amplitude signals are accumulated at the bearing element pass zone. The highest amplitude of the vibration signals has been detected at 798 Hz with the amplitude of 0.44 m/s² that was excited by a gear frequency of $97 \times f_{bsf}$ with respect to Table 3. The second dominant vibration signal has occurred at 740 Hz, which is a natural frequency excited by $90 \times f_{bsf}$. The third dominant signal has been investigated at a pinion frequency ($1 \times f_p$) with amplitude of 0.35 m/s² that has been increased from 0.19 m/s² in same load under sufficient oil condition. The fourth dominant signal has been captured at 795 Hz that was excited by a bearing frequency of $483 \times f_c$. The fifth dominant vibration signal has been detected at 838 Hz that was excited by a signal occurred at $509 \times f_c$. The sixth dominant signal has occurred at 782 Hz and was stimulated by a signal at $475 \times f_c$ as well. Except for the third dominant signal, all other vibration signals are the result of resonance phenomena.



a)



b)

Fig. 4 – a) Spectrum domain for condition of insufficient oil with 1 000 g load,
b) thermal inspection for condition of insufficient oil with 1 000 g load.

The sum of the all six dominant amplitudes is 2.15 m/s². Mesh frequency (f_m) is obtained at 132 Hz with the amplitude of 0.1 m/s² which is lower than the condition of sufficient oil under 1 000 g load that is 0.2 m/s². The signal at the second order of mesh frequency was detected at 264 Hz with the amplitude of 0.03 m/s². The amplitude of $2 \times f_m$ is lower than $1 \times f_m$ which means there is not any excessive misalignment on the gear system. It is assumed that misalignment was corrected while decomposition of the gearbox in removal process of the oil.

Table 3

Dominant frequencies in condition of insufficient oil with 1 000 g load (s: signal)

1.S	2.S	3.S	4.S	5.S	6.S
f_n ($97 \times f_{bsf}$)	f_n ($90 \times f_{bsf}$)	$1 \times f_p$	f_n ($483 \times f_c$)	f_n ($509 \times f_c$)	f_n ($475 \times f_c$)

Under the condition of insufficient oil with 1 000 g load, the waterfall data shows that high-amplitude vibrations are cumulated between 400 Hz and 500 Hz. Some peaks also can be seen around 150 Hz and 750–800 Hz band. Thermal heat distribution and actual temperatures are indicated on vibration measurement points in Fig. 4b. The highest temperature has been detected on the gearbox as 50.1 °C in Fig. 4b. The measured temperature of bearing 1 with 37.3 °C is higher than the measured temperature of bearings 2, 3, and 4. The belt temperature has increased more prominently in comparison with sufficient oil conditions under 250 g and 1 000 g loads.

The temperature of the belt is 36.4 °C which is close to temperature of the bearing 1 and higher than the temperature of bearings 2, 3, 4. The temperature of the plate increased higher than previous test conditions as well; the temperature of the plate is 33 °C and very close to the temperature of bearings 3 and 4.

4. FINDINGS

This part gives overall findings and interpretation of the experiments. Vibration findings are presented with the definition of the dominant signals in the X, Y, Z axes and a sum of the amplitudes are presented as SX, SY, SZ in each axis as well. Thermal findings are with charts of temperature and infrared distribution.

a. Vibrational findings. Vibration charts are given on the X, Y, and Z axes in Fig. 5. Amplitudes are presented in these charts with the vibration acceleration. With respect to Fig. 5, signal amplitude at the fundamental frequency ($1 \times f_p$) of pinion element has been detected as the most dominant in the X axis through sufficient and insufficient oil condition as the load increased to 1 000 g. The most dominant signal detected in the Z axis; and the third dominant signal in the Y axis under insufficient oil condition with 1 000 g load as well.

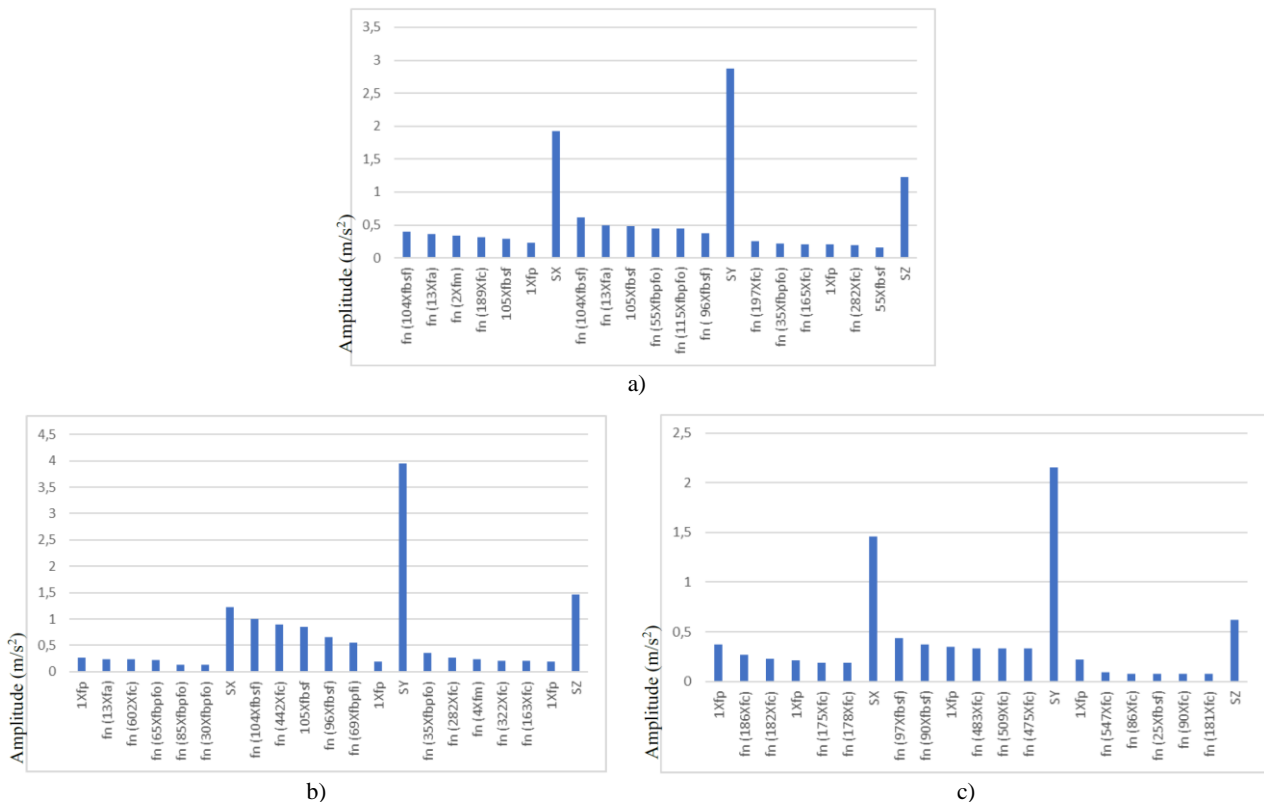


Fig. 5 – Vibration charts: a) condition of sufficient oil with 250 g load; b) condition of sufficient oil with 1000 g load; c) condition of insufficient oil with 1000 g load.

Fundamental frequency ($1 \times f_p$) of pinion element appeared in X axis at sixth dominant signal and Z axis at fourth dominant signal under sufficient oil with 250 g load. Three gear frequencies in X axis, one gear

frequency in *Y* axis and one gear frequency in *Z* axis has been detected under sufficient oil condition with 250 g load. Two gear frequencies in *X* axis, one gear frequency in *Y* axis and two gear frequencies in *Z* axis has been detected under sufficient oil condition with 1 000 g load. Two gear frequencies in *X* axis, one gear frequency in *i* axis and one gear frequency in *Z* axis has been detected under insufficient oil condition with 1 000 g load. It is found that insufficient oil condition affected the bearing frequencies and many signals have been appeared dominantly at the bearing element pass zone. Total number of cage frequencies in six dominant signals are increased in condition of insufficient oil at 1 000 g load. The highest difference between the sum of signal amplitudes in *Y* axis (*SY*) and sum of signal amplitudes in *X* axis (*SX*), *Z* axis (*SZ*) has been detected under sufficient oil condition with 1 000 g.

b. Thermal findings. Temperature changes are given in Table 4 and thermal charts are given in Fig. 6 and Fig. 7.

Table 4

Temperature changes at setup components with respect to the test conditions

CONDITION	LOAD (g)	Gearbox	Motor	Plate	Belt	Bearing 1	Bearing 2	Bearing 3	Bearing 4	Sum
		(°C)	(°C)	(°C)	(°C)	(°C)	(°C)	(°C)	(°C)	(°C)
Sufficient oil	250	37.1	32.1	20.8	27.2	24.6	21.7	22.1	21.5	207.1
	1000	37.7	33.2	22.8	27.4	25.4	23.7	23.7	23.2	217.1
Insufficient oil	1000	50.1	45.2	33	36.4	37.3	34.9	33.5	32.9	303.3

The highest temperature rise has been obtained at bearing 2 from 21.7 °C to 23.7 °C and at plate as well from 20.8 °C to 22.8 °C in comparison of sufficient oil condition under 250 g and 1 000 g with respect to Table 4. The lowest temperature increase has been detected at belt from 27.2 °C to 27.4 °C. The sum of the specified component temperatures has been increased from 207.1 °C to 217.1 °C in conditions of sufficient oil. Temperature on gearbox increased slightly between two conditions from 37.1 °C to 37.7 °C. The temperature increase on bearing 1 has been observed less than bearings 2, 3, and 4. The highest increase is detected at gearbox from 37.7 °C to 50.1 °C as the difference is 12.4 °C in comparison on sufficient oil and insufficient oil with 1 000 g load. Second highest increase has been obtained at electrical motor from 33.2 °C to 45.2 °C with the difference of 12 °C. Sum of the specified components has been increased from 217.1 °C to 303.3 °C. The temperature increase on bearing 1 has been observed higher than bearings 2, 3, and 4.

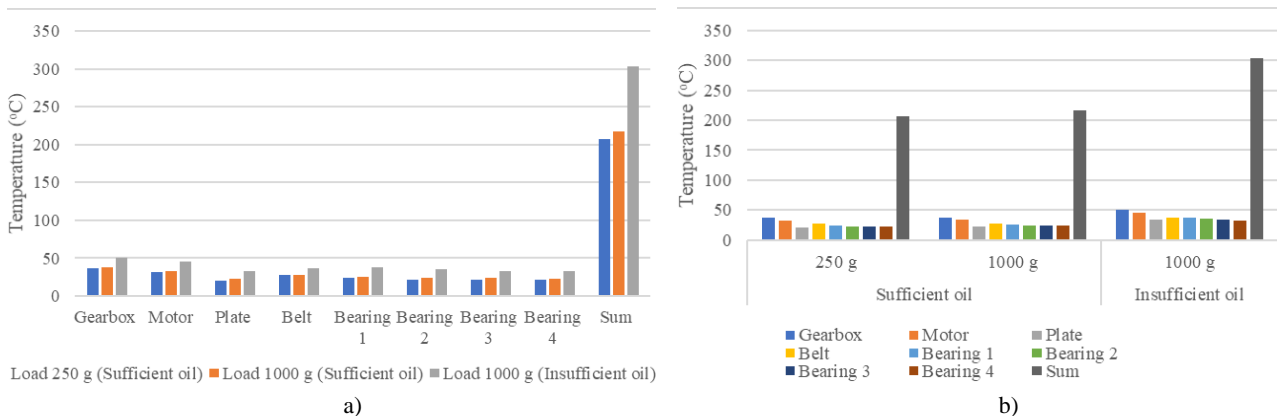


Fig. 6 – Temperature charts: a) load and oil sufficiency; b) setup components.

Figure 6 shows that there is almost no temperature difference in gearbox, belt and bearing 1 under sufficient oil conditions with loads of 250 g and 1 000 g. There is a slight increase in motor, plate, bearings 2, 3, and 4 under same test conditions. All bearings' temperatures have been increased and stabilized at a similar temperature range in sufficient and insufficient oil conditions.

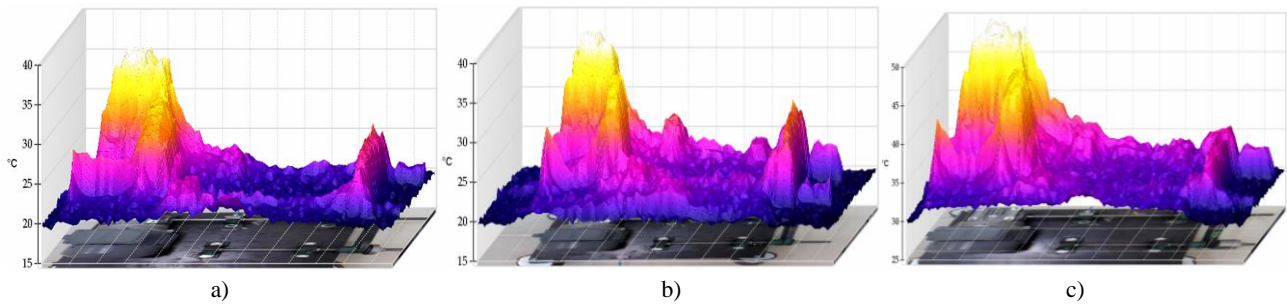


Fig. 7 – Infrared thermal distributions; a) 250 g load under condition of sufficient oil, b) 1000 g load under condition of sufficient oil, c) 1000 g load under condition of insufficient oil.

The sum of the overall temperatures in insufficient oil has been increased dramatically around 100 °C with respect to sums of sufficient oil test conditions. The highest temperature has been observed at gearbox in all of sufficient and insufficient test conditions. Bearing 1 has reflected higher temperature increase than the belt temperature in comparison with sufficient oil conditions.

Infrared thermal distributions over test setup in tested conditions are given in Fig. 7. Oil starvation has been conditioned in the gearbox; heat is increased higher than the infrared distribution with 1 000 g load under condition of sufficient oil. Temperature on bearing has been reached higher than 35 °C. Overall heat is increased on test setup components respect to the color change. Especially heat on bearing 1 is more prominent in comparison with infrared distribution with 250 g load under condition of sufficient oil. Maximum temperature increased over 40 °C as well through gearbox component. Heat over belt and electrical motor has been increased as well. Heat distribution is mainly with yellow, red, pink colors in increase on gearbox partly on the one side of electrical motor and the belt in Fig. 7. Moreover, heat is distributed from gearbox to bearing as well.

5. RESULTS AND CONCLUSIONS

This research investigated the condition monitoring of a worm-type gearbox by vibro-thermal analysis with respect to the oil starvation under variable loads. The tests were conducted on a test setup in laboratory conditions, and the data were analyzed using a tribo-prognostic approach.

The vibration signal at pinion frequency occurred as the most dominant amplitude with respect to the increase in the load from 250 g to 1 000 g in the tests. That most dominant amplitude was detected in the X axis for the 1 000 g load with sufficient oil and in the X, Z axes for the 1 000 g load with insufficient oil. The frequency spectra did not show a significant difference under the 250 g and 1 000 g loads in the sufficient oil conditions. Three signals were at the same frequencies f_n ($104 \times f_{bst}$), $105 \times f_{bst}$, and f_n ($96 \times f_{bst}$) among six dominant amplitudes in both conditions. The sum of the amplitudes in the Y, Z axes increased and the X axis decreased under the 1 000 g load in comparison with 250 g. Spectrum domain showed a radical change in the insufficient oil conditions under the 1 000 g load. The sum of the amplitudes in the Y, Z axes decreased and the X axis increased under the 1 000 g load in insufficient oil conditions in comparison with the 1 000 g load in sufficient oil conditions. That is the consequence of the distribution of overall vibration energy through the increase in the amount of signals that occurred on the frequency domain with respect to the excitation of natural frequencies due to frictional forces based on oil starvation. With respect to the Y axis results, none of the common signal frequencies were detected with 250 g load and one common frequency was detected with 1 000 g load at $1 \times f_p$. The oil starvation conditions for the gearbox had caused a similar effect on the bearing; and cage frequencies became more dominant.

The temperature differences increased gradually with respect to load increase and oil starvation in tested conditions. The overall temperature at the vibration measurement points increased 10 °C in the tested sufficient oil conditions and increased 86.2 °C in the insufficient oil conditions under 1 000 g load in comparison with the same load in the sufficient oil conditions. The temperature of the gearbox increased 0.6 °C in sufficient oil conditions and 12.4 °C in insufficient oil conditions under 1 000 g load in comparison with the same load in sufficient oil condition. The heat increase was significant due to oil starvation

conditions and can be diagnosed clearly with the thermal data gathered; otherwise, it was not significant in sufficient oil conditions. The thermal distribution was spread from high to low mainly from the gearbox to other parts of the test setup in insufficient oil conditions.

Conditions of oil sufficiency with tested loads can be monitored by vibration analysis. Overall vibration energy of the system may get distributed through the amount of vibration signals caused by frictional points under insufficient oil conditions in worm-type gearboxes. Thermal analysis augments vibration analysis with respect to detection of deficiencies and ease of diagnosing components of the overall system. The threshold levels can be determined in both vibration and thermal analysis in order to build an early warning system. Consequently, vibro-thermal analysis is an approach that brings the capabilities of vibration and thermal analysis together in paired usage.

This research suggests that condition monitoring of worm-type gearboxes with a tribo-prognostics approach through vibro-thermal analysis may make maintenance more cost-effective, decrease the maintenance duration and improve the quality of maintenance when it is implemented in real practices.

ACKNOWLEDGEMENTS

Thanks to Kilis 7 Aralik University Scientific Research Projects Coordination Unit project no: 16-10848 and to The Scientific and Technological Research Council of Turkey (TUBITAK) for contributions to this study.

REFERENCES

1. G.S. LAMANI, N.G. RANALKAR, O.P. PAWAR, S.V. PATIL, *Vibration analysis of worm and worm wheel gearbox*, International Journal of Mechanical, Robotics and Production Engineering, **7**, pp. 81-84, 2018.
2. H. XIAO, X. ZHOU, J. LIU, Y. SHAO, *Vibration transmission and energy dissipation through the gear-shaft bearing-housing system subjected to impulse force on gear*, Measurement, **102**, pp. 64-79, 2017.
3. A.S. SAIT, Y.I. SHARAF-ELDEEN, *A review of gearbox condition monitoring based on vibration analysis techniques diagnostics and prognostics*, Rotating Machinery, Structural Health Monitoring, Shock and Vibration, **5**, pp. 307-324, 2011.
4. A. MAURICIO, C. FREITAS, J. CUENCA, B. CORNELIS, K. JANSSENS, *Condition monitoring of gears under medium rotational speed*, 24th International Congress on Sound and Vibration, 2017.
5. S.B. GHODAKE, A.K. MISHRA, A.V. DEOKAR, *A review paper on fault detection of worm gearbox*, International Advanced Research Journal in Science, Engineering and Technology, **3**, Special Issue 1, pp. 307-324, 2016.
6. S. AL-ARBI, *Condition monitoring of gear systems using vibration analysis*, PhD thesis, University of Huddersfield, 2012.
7. P. VECER, M. KREIDL, R. SMID, *Condition indicators for gearbox condition monitoring systems*, Acta Polytechnica, **45**, 6, pp. 35-43, 2005.
8. J. YIN, W. WANG, Z. MAN, S. KHOO, *Statistical modeling of gear vibration signals and its application to detecting and diagnosing gear faults*, Information Sciences, **259**, pp. 295-303, 2014.
9. A.D. NEMBARD, J.K. SINHA, A.J. PINKERTON, K. ELBHBAH, *Combined vibration and thermal analysis for the condition monitoring of rotating machinery*, Structural Health Monitoring, **13**, 3, pp. 281-295, 2014.
10. E. RESENDIZ-OCHOA, J.J. SAUCEDO-DORANTES, J.P. BENITEZ-RANGEL, R.A. OSORNIO-RIOS, L.A. MORALES-HERNANDEZ, *Novel methodology for condition monitoring of gear wear using supervised learning and infrared thermography*, Applied Sciences, **10**, 2, pp. 1-18, 2020.

Received May 13, 2020